

A method for model-reduction of non-linear thermal dynamics of multi-zone buildings[☆]

Siddharth Goyal, Prabir Barooah*

Department of Mechanical and Aerospace Engineering, University of Florida, Gainesville, FL 32611, USA

ARTICLE INFO

Article history:

Received 29 July 2011

Received in revised form

26 November 2011

Accepted 8 December 2011

Keywords:

Building thermal dynamics

Non-linear model reduction

Reduced-order modeling

Thermal modeling

ABSTRACT

We propose a method for reducing the order of dynamic models of temperature and humidity in multi-zone buildings. Low-order models of building thermal dynamics are useful for model-based HVAC control techniques, especially to computationally intensive ones such as Model Predictive Control (MPC). Even a lumped parameter model for a multi-zone building, which is a set of non-linear coupled ordinary differential equations, can have large state-space dimension. Model reduction techniques are useful to simplify such models. Although there are a number of well-developed techniques for model reduction of linear systems, techniques available for non-linear systems are limited. The method we propose exploits the linear portion of the model to compute a transformation (by using balanced realization) and a specific sparsity pattern of the non-linear portion that building thermal models possess to obtain the reduced order model. Simulations show that the prediction of the zone temperatures and humidity ratios by the reduced model is quite close to that from the full-scale model, even when substantial reduction of model order is specified that reduces computation time by a factor of six or more.

© 2011 Elsevier B.V. All rights reserved.

1. Introduction

Buildings are one of the primary consumers of energy worldwide, and particularly in the United States. Inefficiency in the building technologies, particularly in operating the HVAC (heating, ventilation and air conditioning) systems cause a significant fraction of energy consumed by building to be wasted. Part of the reason is that HVAC systems are operated on a pre-designed schedule of zone-wise temperature set points that zonal PID (proportional integral derivative) controllers try to maintain. To improve energy efficiency, there is a growing interest in developing techniques that compute control signals that minimize building-wide energy consumption [1–5]. Such control techniques require a model of the transient thermal dynamics of the building that relates the control signals to the space temperature and humidity of each zone.¹

A model of the transient thermal dynamics of a multi-zone building can be constructed from energy and mass balance equations. An attempt to model all the relevant physical phenomena

will lead to a set of coupled partial differential equations. Prediction using such a model is computationally demanding due to the complexity of the model. However, an important requirement of a dynamic model for use in real-time control is simplicity, since overly complex models with large state spaces will render them too slow for prediction in real-time. Therefore, one has to use simplified, i.e., *reduced order*, models. In such a model, the air in a zone is assumed to be well-mixed so that each zone is characterized by a single temperature. Resistor–capacitor (RC) networks are commonly used for constructing a reduced order model of the transient heat flow through a solid surface, such as a wall [6,7]. The resistances and capacitances are carefully chosen to model the combined effect of conduction between the air masses separated by the surface, as well as long wave radiation and convection between the surface and the air mass in contact with it [[6,8],[9, Chapters 3, 29, and 31]]. A RC network model of a solid surface is a set of linear differential equations whose order is equal to the number of capacitors. The heat and moisture exchanged between a zone and the outside due to the air supplied and extracted by the HVAC system can be modeled with ordinary differential equations (ODEs). These are non-linear ODEs if the latent heat of the humid air is taken into account. Assuming thermal interaction among zones due to convection is negligible, a dynamic model of a multi-zone building can be constructed by linking the linear ODEs corresponding to the RC networks for the solid surfaces and the non-linear ODEs corresponding to the moist air enthalpy dynamics. This results in a system of coupled ODEs. We call such a model a *full-scale* model,

[☆] This work has been supported by the National Science Foundation by Grants CNS-0931885 and ECCS-0955023.

* Corresponding author.

E-mail addresses: siddgoya@ufl.edu, siddgoya@gmail.com (S. Goyal), pbarooah@gmail.com (P. Barooah).

¹ In this paper we use “humidity ratio” to measure humidity, which is the ratio of mass of water vapor to the mass of dry air.

Nomenclature

$\omega_{\text{H}_2\text{O}}$	rate of water vapor released by a person due to respiration (kg/s)
C_{ij}	thermal capacitance of a node internal to a wall that connects zone i and j , and closer to zone i (kJ/K)
C_i	thermal capacitance of i th zone (kJ/K)
C_{pa}	specific heat capacity of air at constant pressure = 1.006 (kJ/(kg °C))
C_{pw}	specific heat capacity of water vapor at constant pressure = 1.84 (kJ/(kg °C))
h^{in}	enthalpy of supply air (kJ/kg)
h^{out}	enthalpy of air being exhausted out of a zone (kJ/kg)
h_{we}	evaporation heat of water at 0 °C = 2501 (kJ/kg)
m^{in}	mass flow rate of supply air (kg/s)
m^{out}	flow rate of air being exhausted out of a zone (kg/s)
N	number of zones
n^p	number of people
p^{da}	partial pressure of dry air (atm)
Q^p	rate of heat gain due to occupants, lightning, etc. (kW)
Q^s	rate of heat gain due to solar radiation (kW)
R_g	specific gas constant of dry air = 287.04 (J/(kg K))
$R_{i,j}, R_{i,j}^{\text{mid}}$	thermal resistances of part of a wall that connects zone i and j (K/W)
T	temperature (°C)
T^{supply}	temperature of air supplied by AHU (°C)
T_0	outside temperature (°C)
V	volume of air in the zone (m ³)
W	humidity ratio
W^{in}	humidity ratio of supply air
W^{supply}	humidity ratio of air supplied by AHU
subscript i	i th zone, $i = 1, \dots, N$

which are explained in detail in the next section. If lumped parameter models of inter-zone convective heat transfer are available, they can be included in the full-scale model as well. Some preliminary work on modeling inter-zone convection with the help of RC networks is reported in [10].

The states of the full-scale model consist of not only zone temperatures and humidities but also temperatures of “nodes” that are internal to walls, ceiling and floors, which arise due to the RC network models of these surfaces. Even though the full-scale model itself is a simplified, lumped-parameter model, it suffers from large state space dimension even for a moderate number of zones. For instance, a 4-zone building model may have a state-space dimension of 40 or more, and a building with 100 zones may have a state-space dimension of a thousand. Thus, such a model is not suitable for a model-based control technique, especially ones such as MPC (Model Predictive Control) that requires on-line optimization based on model prediction.

In this paper, we propose a method for reducing the order of a full-scale model of the thermal dynamics of a multi-zone building. In model reduction, one seeks to maintain the accuracy of the prediction of outputs from inputs while reducing the number of states. We choose outputs as space temperatures and humidities of the zones. The inputs are outside temperature and humidity, heat gains from occupants and solar radiation, and supply air flow rates and supply air temperatures.

The full-scale model is a set of non-linear coupled ODEs (ordinary differential equations) that are obtained by mass and energy balance. There are a number of well-developed techniques for model reduction of linear systems; see [11] for a review. However, model reduction of non-linear systems is a less developed

area. Some work has been done on model reduction of bilinear systems [12–15]. Since the full-scale model we consider is not bilinear, these methods are not applicable. Other notable work on non-linear model reduction includes the energy-function based method of [16], the empirical Gramian based method of [17], and its extension in [18] to systems with non-zero steady impulse response. The proposed method avoids the computational difficulties in obtaining the energy function that is required by the method of [16]. Though the method proposed in [17] is quite general since it does not require any specific structure of the full-scale model, it requires collecting extensive and sufficiently rich simulation data to construct the so-called empirical Gramians. In addition, being developed for a fully general non-linear model, this method is unable to take advantage of any specific structure that a particular system may possess. The interested reader is referred to [18] for a review – as well as a comparison of merits and weaknesses – of existing non-linear model reduction techniques.

In the method proposed here, we exploit a specific structure of the model that is unique to multi-zone building thermal dynamics and existing model reduction techniques for LTI systems to reduce the model order. The non-linear full-scale model is a combination of a LTI (linear-time-invariant) component and a non-linear component. The LTI component comes from the RC network models of conduction through solid surfaces of the building, such as walls, windows, floors and ceilings, while the non-linear part is due to the enthalpy exchange between a zone and ventilation air. Since ventilation air does not *directly* affect the internal temperature of the walls, the non-linear terms on the right hand side of the ODE $\dot{x} = f(x, v)$ only appear in a small number of states, the dynamics of the other states appear linearly. The proposed method exploits this sparsity of the non-linear terms: first a coordinate transformation is computed in such a way that the linear part of the model is balanced, i.e., its controllability and observability Gramians are equal and diagonal. Then the same transformation is applied to the non-linear part as well. Since the nonlinear portion has a sparse pattern, it is possible to truncate the states of full scale model. The proposed method is therefore uniquely suited to order reduction of building thermal dynamics, or to any coupled ODE model that has the aforementioned sparsity structure. In contrast, the model reduction methods for non-linear systems mentioned above – even if they are applicable to building thermal dynamics – do not take advantage of the special structure of the thermal dynamics. Although here we use balanced realization to compute the transformation, other methods of linear model reduction that lead to a state transformation of the LTI part, such as [19], may be used as well. The number of outputs in the full-scale model is $2N$ for a N -zone building (temperatures and humidities of the N zones). Therefore the state dimension of the reduced model, though user-specified, has a minimum possible value of $2N$.

The proposed model reduction method is applicable to a building as long as the full-scale model is applicable. Since the full-scale model is based on mass and energy balance at each zone due to conduction through walls and enthalpy exchange due to ventilation, we expect that the thermal dynamics of most commercial and residential buildings can be modeled this way, in particular, those employing CAV (constant air volume) or VAV (variable air volume) systems.

Simulation results show that the space temperature and humidity ratio prediction by the reduced model is quite close to the prediction by the full scale model. Furthermore, reducing model order can reduce the computation time significantly. When the model order is reduced from 40 states to 14 states, the rms error in the temperature predictions are seen to be 0.5 °C over a period of 24h, with the maximum error of 2.9 °C. The maximum error appears during initial transients. The rms and maximum error in the humidity ratio predictions are 1.4×10^{-4} and 16×10^{-4} ,

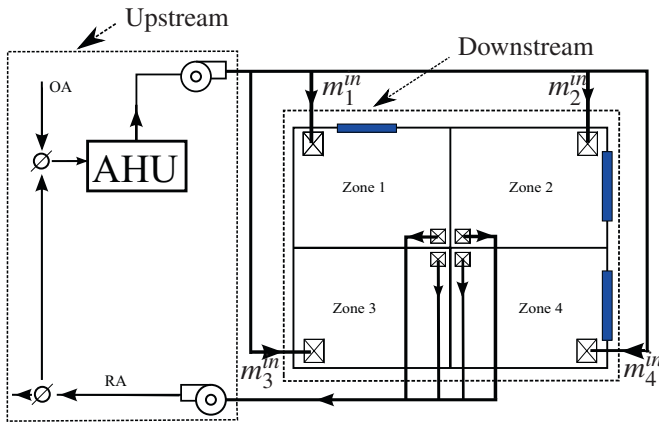


Fig. 1. A schematic of a 4-zone building and its HVAC system.

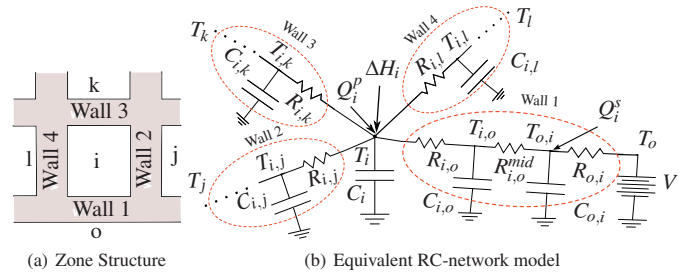


Fig. 2. A lumped RC-network model for conductive interaction between the zones o, i, j, k and l , where o represents the outside zone. For simplicity, we have not shown the floor and the ceiling, but can be included in general.

which are 1.6% and 18% of the predictions by the full-scale model, respectively. The maximum error only occurs in the first 20 min; after that the error is around 1%. It is known that reducing model order increases the error in predictions. When the same model is reduced to an 8th order model, its minimum possible state dimension, the rms and peak error in the temperature predictions increase to 2 °C and 9.7 °C. However, errors in the humidity ratio predictions are same as when the model order is reduced to 14. Again, the large maximum errors occur in the initial transients. The computation time is reduced by a factor of 6. Since the focus of the paper is model reduction and not model construction/calibration, we only compare the predictions of the reduced-order model to that of a full-scale model, not with measured data.

The rest of the paper is organized as follows. Section 2 describes briefly the non-linear model of building thermal dynamics. The proposed method for order reduction of this model is described in Section 3. Results from numerical simulations are presented in Section 4.

2. Full-scale model of building thermal dynamics

Before getting to model reduction, we first describe the full-scale model including its inputs, outputs and state variables, and the assumptions involved in constructing it. Although a number of papers on thermal modeling of buildings exist, quite a few of them are limited to single zones [20–22] or a very small number of zones [23]. The papers [4,5,24] model conduction between multiple zones, but do not model the non-linear effects of humidity on the temperature response. The paper by Wang [25] presents a full-scale non-linear model of multi-zone buildings with an arbitrary number of zones with a model of inter-zone convection based on temperature difference. However, Wang also does not take into account the non-linear effect of moist air on temperature, and moreover uses a 1R1C model for conduction among zones. It has been shown that 1R1C – or even 2R1C – models are less accurate than 3R2C models in predicting temperature response, and that 3R2C models represent the best compromise between prediction accuracy and model complexity [6]. Use of 3R2C models instead of 1R1C models increases the model order by a factor of two, creating a greater need for model reduction.

A schematic of a building with four zones and its associated HVAC system is shown in Fig. 1. To predict zone temperatures and humidities, the full-scale model takes the following variables as external inputs: (i) characteristics of the supply air (flow rate, temperature and humidity) into each zone, (ii) thermal heat gain due to occupants (body heat, heat released by equipments and lights) of each zone, (iii) thermal heat gain of each zone due to solar radiation,

and (iv) outside temperature. Note that some of the inputs, namely, characteristics of the supply air, depend on the commands to the air handling unit (AHU), such as fan speed, and chilled water flow rate. In this paper, we ignore the “upstream” side of the dynamics that includes the AHU, and concentrate on modeling the “downstream” side (see Fig. 1). The reason for ignoring the upstream side, which includes the AHU dynamics, is twofold. First, the size of the downstream model increases fast with the number of zones, but the size of the upstream model increases only with the number of AHUs. Even for a large building the number of AHUs is typically small. For instance, a 66-zone building at the University of Florida campus has 3 AHUs. Thus, the downstream model requires model reduction techniques much more than the upstream model. Second, the AHU has the fastest dynamics in the HVAC system, with a time constant of about a minute [26], whereas the thermal dynamics of the zones are far slower with time constants in the order tens of minutes [20] to hours [7]. As a result, it may be possible to replace the dynamics of the AHUs and ducts by static gains without losing too much accuracy.

In the full-scale lumped parameter model the air in each zone (which can be a room, several rooms, or a partitioned space in a room) is assumed to be well mixed, so that there is one temperature and humidity value associated with each zone. The variables of interest that the model is required to predict are T_1, \dots, T_N and W_1, \dots, W_N . The humidity ratio of a volume of moist air is defined as the ratio of the mass of water present in the air to the mass of dry air. The vector v of input signals to the building thermal dynamics, which consists of flow rate, temperature and humidity of supply air, outside temperature, heat gain due to the occupants, lightning and solar radiation is defined below ($i = 1, \dots, N$).

$$v = [m_1^{\text{in}}, \dots, m_N^{\text{in}}, W_1^{\text{in}}, \dots, W_N^{\text{in}}, T_1^{\text{in}}, \dots, T_N^{\text{in}}, Q_1^{\text{p}}, \dots, Q_N^{\text{p}}, Q_1^{\text{s}}, \dots, Q_N^{\text{s}}, T_0]^T, \quad (1)$$

Often $T_i^{\text{in}} = T^{\text{supply}}$ and $W_i^{\text{in}} = W^{\text{supply}}$ for all i . As discussed in Section 1, only conductive heat transfer among zones, and heat exchange due to supply and return air, is considered in the model. Inter-zone convection is ignored. We use 3R2C circuits to model conduction, where a solid surface separating two volumes of air is modeled by a network of three resistors and two capacitors [6,7]. Each zone also has an associated capacitance that models the heat capacity of the air in the zone as well as that of the furniture, etc., in it.

Consider the example shown in Fig. 2: zone i is separated by walls to zone j, k, l , and the outside, which is denoted by o . For ease of description we do not include the floor and the ceiling in this example. Recall that the parameter C_i is the capacitance of zone i and $R_{i,o}, R_{i,o}^{\text{mid}}, R_{o,i}$ and $C_{i,o}, C_{o,i}$ are the resistances and capacitances, respectively, corresponding to the 3R2C model of the wall separating zone i from the zone o . When each wall is modeled as a 3R2C network, the dynamics of T_i , the temperature of zone i , becomes

$$C_i \dot{T}_i = - \left[\frac{1}{R_{i,o}} + \frac{1}{R_{i,j}} + \frac{1}{R_{i,k}} + \frac{1}{R_{i,l}} \right] T_i + \frac{T_{i,o}}{R_{i,o}} + \frac{T_{i,j}}{R_{i,j}} + \frac{T_{i,k}}{R_{i,k}} + \frac{T_{i,l}}{R_{i,l}} + Q_i^p + \Delta H_i, \quad (2)$$

The term ΔH_i is the net gained by the zone due to supply and extracted air, which will be described in more detail soon. The dynamic equations for the variables $T_{i,o}, T_{o,i}$, which are the temperatures of the “internal” nodes of the wall separating i and o , are:

$$C_{i,o} \dot{T}_{o,i} = - \left[\frac{1}{R_{o,i}} + \frac{1}{R_{i,o}^{mid}} \right] T_{o,i} + \frac{T_{i,o}}{R_{i,o}^{mid}} + \frac{T_o}{R_{o,i}} + Q_i^s$$

$$C_{o,i} \dot{T}_{i,o} = - \left[\frac{1}{R_{i,o}^{mid}} + \frac{1}{R_{i,o}} \right] T_{i,o} + \frac{T_i}{R_{i,o}} + \frac{T_{o,i}}{R_{i,o}^{mid}} \quad (3)$$

The values of the three resistances and two capacitances for a wall can be computed from the material properties and geometry of the wall, which determines its total resistance and capacitance, and then applying the formulas specified by Gouda et al. [6] that splits the total capacitance into two capacitances and the total resistance into three resistances. Windows are modeled as single resistors since they have negligible capacitance as compared to the walls.

The term ΔH_i in (2) due to the enthalpy of the supply and extract air is

$$\Delta H_i = m_i^{in} h_i^{in}(T_i^{in}, W_i^{in}) - m_i^{out} h_i^{out}(T_i, W_i), \quad i = 1, 2, \dots, N. \quad (4)$$

For the sake of simplicity we ignore infiltration; it can be included if desired in (4). The enthalpies $h_i^{(\cdot)}$ in (4) can be computed from psychometric equations [9] as

$$h_i^{in} = C_{pa} T_i^{in} + W_i^{in}(h_{we} + C_{pw} T_i^{in}) \quad (5)$$

$$h_i^{out} = C_{pa} T_i + W_i(h_{we} + C_{pw} T_i) \quad (6)$$

Note that the flow rate of moist air leaving zone i is $m_i^{out}(t) = m_i^{in}(t) + n_i^p(t)\omega_{H_2O}$. It is assumed that air leaving the zone has the same temperature and humidity ratio as air present in the zone. The humidity dynamics can be derived from mass balance and gas laws as

$$\frac{dW_i}{dt} = \frac{R_g T_i}{V_i P_{da}} \left[n_i^p \omega_{H_2O} + m_i^{in} \frac{W_i^{in} - W_i}{1 + W_i^{in}} \right], \quad i = 1, 2, \dots, N. \quad (7)$$

Detailed derivation of (7) is included in ***Appendix A. Again, we have neglected exfiltration/infiltration in deriving (7) for the sake of simplicity. The full-scale model of the entire building’s thermal dynamics can now be constructed by collecting Eqs. (2)–(7) for all the zones $i = 1, \dots, N$ as well as Eq. (3) corresponding to the internal “nodes” in the RC networks for all the solid surfaces (walls, windows, floors, ceilings). It is convenient to associate every temperature variable (except for the supply air and outside air temperatures) with a unique node. The total number of nodes in the model of a N zone building, which is denoted by n , is

$$n = N + N_{int},$$

where N_{int} is the number of nodes that corresponds to the temperatures inside solid surfaces.² The full-scale model is obtained by

² If one needs to account for variations of outside air temperatures on different sides of a building, more than one outside temperatures are needed as inputs. This can be easily done but we refrain from describing it since it makes the notation more complex.

collecting the coupled ODEs for node temperatures and humidity ratios, expressed compactly as

$$\dot{T} = AT + BU + f(T, W, v), \quad (8)$$

$$\dot{W} = g(T, W, v) \quad (9)$$

where $T \triangleq [T_1, \dots, T_N, \dots, T_n]^T \in \mathbb{R}^n$ contains the temperatures of the nodes, $U \triangleq [T_o, Q_1^p, \dots, Q_N^p, Q_1^s, \dots, Q_N^s]^T$ is a sub-vector of the input vector v as defined in (1), and $W \triangleq [W_1, W_2, \dots, W_N]^T$, $f(T, W, v) \triangleq [\Delta H_1, \Delta H_2, \dots, \Delta H_N, 0, \dots, 0]^T \in \mathbb{R}^n$. The entries of the matrices $A \in \mathbb{R}^{n \times n}$ and $B \in \mathbb{R}^{n \times (2N+1)}$ are determined by the resistances and capacitances corresponding to each solid surface, as well as the capacitances of the zones.

We have indexed the nodes so that the first N components of the state vector T correspond to the space temperature of N zones, and remaining $n-N$ states correspond to the internal node temperatures of the surface elements. As a result, f has a special structure; only its first N entries are potentially non-zero, which correspond to the heat gain in the N zones. The remaining entries of f are zeros. This fact will be useful in the proposed model reduction method, which is presented next.

3. Model reduction method

We start with a brief review of the classical balanced truncation method of model reduction of linear time invariant (LTI) systems; more details can be found in [28–31]. Balanced truncation is used in reducing the order of the full-scale non-linear building thermal model.

3.1. Review of balanced truncation method for LTI system

Consider a stable linear time invariant (LTI) system with a $p \times m$ transfer function $G(s)$, i.e., with m inputs and p outputs. Suppose it has a state-space realization

$$\dot{x} = Ax + Bu, \quad y = Cx + Du \quad (10)$$

where $x \in \mathbb{R}^n$ is the state vector, $u \in \mathbb{R}^m$ is the input vector and $y \in \mathbb{R}^p$ is the output vector. Thus, $A \in \mathbb{R}^{n \times n}$, $B \in \mathbb{R}^{n \times m}$, $C \in \mathbb{R}^{p \times n}$ and $D \in \mathbb{R}^{p \times m}$. The controllability Gramian $G^{(c)}$ and observability Gramian $G^{(o)}$ of (11) are defined as

$$G^{(c)}(A, B) \triangleq \int_0^\infty e^{At} B B^T e^{A^T t} dt, \quad G^{(o)}(A, C) = \int_0^\infty e^{A^T t} C^T C e^{At} dt.$$

Consider a transformation $x_b = Rx$ which gives us the transformed realization

$$\dot{x}_b = A_b x_b + B_b u, \quad y_b = y = C_b x_b + Du, \quad (11)$$

where $A_b = RAR^{-1}$, $B_b = RB$, and $C_b = CR^{-1}$.

This is called a balanced realization if R is chosen in a way that the controllability and observability Gramians $G_b^{(c)}, G_b^{(o)}$ of (11) are both equal and diagonal:

$$G_b^{(c)} = G_b^{(o)} = \begin{pmatrix} \lambda_1 & 0 & 0 \\ 0 & \ddots & 0 \\ 0 & 0 & \lambda_n \end{pmatrix},$$

where $G_b^{(c)} = G^{(c)}(A_b, B_b)$, $G_b^{(o)} = G^{(o)}(A_b, C_b)$, and where $\lambda_1 > \lambda_2 > \dots > \lambda_n > 0$. Suppose, we want to reduce the full-scale n th order LTI system (10) to a q th order LTI system, with $q < n$. Decompose A_b, B_b, C_b as

$$A_b = \begin{bmatrix} A_{11} & A_{12} \\ A_{21} & A_{22} \end{bmatrix}, \quad B_b = [B_1^T \quad B_2^T]^T, \quad C_b = [C_1 \quad C_2]$$

where $A_{11} \in \mathbb{R}^{q \times q}, A_{12} \in \mathbb{R}^{q \times (n-q)}, A_{21} \in \mathbb{R}^{(n-q) \times q}, A_{22} \in \mathbb{R}^{(n-q) \times (n-q)}, B_1 \in \mathbb{R}^{q \times m}, B_2 \in \mathbb{R}^{(n-q) \times m}, C_1 \in \mathbb{R}^{p \times q}$ and $C_2 \in \mathbb{R}^{p \times (n-q)}$.

Define $x_q \triangleq [I_{q \times q} \quad 0_{q \times (n-q)}] x_b$, which is a vector in \mathbb{R}^q consisting of first q entries of x_b . The system

$$\dot{x}_q = A_{11}x_q + B_1u, \quad y_q = C_1x_q + Du$$

is a reduced model (of order q) of the full n th order model (10), where states corresponding to the $n - q$ smallest eigenvalues of $G_b^{(c)}$ and $C_b^{(o)}$ are ignored. This method of obtaining a reduced order model of a LTI system is called balanced truncation.

3.2. A balanced truncation-like reduction of nonlinear building thermal model

We now describe the proposed model reduction method. The goal is to approximate the non-linear ODEs (8) and (9) by another, smaller set of ODEs with minimal loss of predictive power. We focus on reducing the number of temperature states. Since the humidity ratio state vector W has one variable for every zone, it is left untouched. Recall that the temperature dynamics of the building thermal model is

$$\dot{T} = AT + BU + f(T, W, v), \tag{12}$$

where $T \in \mathbb{R}^n$ contains the n temperature states. Due to the way in which the entries of T are indexed, we can write it as

$$T = [T_z^T, \quad T_{nz}^T]^T, \tag{13}$$

where $T_z \triangleq [T_1 \quad T_2 \dots T_N]^T$ is the vector of zone temperatures and $T_{nz} \in \mathbb{R}^{N_{int}}$ is the vector of the temperatures of the nodes internal to walls. Since all but the first N entries of f are zeros, it can be decomposed as

$$f(T, W, v) = [f_a^T(T_z, W, v) \quad 0_{(n-N) \times 1}^T]^T, \text{ where } f_a \in \mathbb{R}^N, \tag{14}$$

where we are now using the fact that the entries of the vector f only depends on the space temperatures T_z and not on the temperatures of nodes internal to the walls. We now introduce a fictitious output of the following form:

$$Y = CT, \quad Y \in \mathbb{R}^p, p \geq N, \tag{15}$$

where C can be any $\mathbb{R}^{p \times n}$ matrix but with the constraint that Y contains T_z , the vector of zone temperatures, as a sub-vector. That is, with appropriate indexing, Y can be expressed as

$$Y \triangleq \begin{bmatrix} T_z \\ Y_{nz} \end{bmatrix}, \tag{16}$$

where $Y_{nz} \in \mathbb{R}^{(p-N)}$. Combining (12)–(16), we get

$$\begin{bmatrix} \dot{T} \\ \dot{W} \\ Y \end{bmatrix} = \begin{bmatrix} AT + BU + [f_a^T(T_z, W, v) \quad 0_{(n-N) \times 1}^T]^T \\ g(T_z, W, v) \\ CT \end{bmatrix} \tag{17}$$

where we have again used the fact that $g(\cdot)$ only depends on the space temperatures and not on the temperatures of the nodes internal of the walls.

Let $T_b := RT$, where $R \in \mathbb{R}^{n \times n}$ is the co-ordinate transformation that leads to a balanced realization of the system $\dot{T} = AT + BU$, where A, B are the corresponding matrices from (8). Note that such a transformation exists since the LTI part of the full-scale model is stable. Stability follows from the physics of RC networks; we therefore do not provide a proof. The transformation R can be computed

using standard software; e.g., the command `balreal` in MATLAB[®]. Eq. (8)–(9) can now be expressed as

$$\begin{bmatrix} \dot{T}_b \\ \dot{W} \\ Y \end{bmatrix} = \begin{bmatrix} A_b T_b + B_b U + R[f_a^T(T_z, W, v) \quad 0_{(n-N) \times 1}^T]^T \\ g(T_z, W, v) \\ C_b T_b \end{bmatrix} \tag{18}$$

where $A_b = RAR^{-1}, B_b = RB$, and $C_b = CR^{-1}$.

Note that the computation of R is solely based on the LTI part of (8). Let r ($p \leq r < n$) be the desired order of the temperature states of the reduced model. Now we decompose the vector T_b and the matrices A_b, B_b, C_b as:

$$T_b = [T_r^T \quad T_g^T]^T, \quad A_b = \begin{bmatrix} A_{11} & A_{12} \\ A_{21} & A_{22} \end{bmatrix}, \quad B_b = \begin{bmatrix} B_1 \\ B_2 \end{bmatrix} \tag{19}$$

$$C_b = [C_1 \quad C_2], \quad R = \begin{bmatrix} R_{11} & R_{12} \\ R_{21} & R_{22} \end{bmatrix}, \tag{20}$$

where $T_r \in \mathbb{R}^r$ consists of the first r entries of T_b , and $A_{11} \in \mathbb{R}^{r \times r}, A_{12} \in \mathbb{R}^{r \times (n-r)}, A_{21} \in \mathbb{R}^{(n-r) \times r}, A_{22} \in \mathbb{R}^{(n-r) \times (n-r)}, B_1 \in \mathbb{R}^{r \times m}, B_2 \in \mathbb{R}^{(n-r) \times m}, C_1 \in \mathbb{R}^{p \times r}, C_2 \in \mathbb{R}^{p \times (n-r)}$, and $R_{11} \in \mathbb{R}^{r \times r}, R_{22} \in \mathbb{R}^{(n-r) \times (n-r)}$. Now we define f_r as a vector that contains the vector f_a and possibly additional zeros:

$$f_r(T_z, W, v) \triangleq [f_a^T(T_z, W, v) \quad 0_{(r-N) \times 1}^T]^T \in \mathbb{R}^r.$$

We now eliminate the last $n - r$ states of T_b , i.e., set $T_g = 0$. This leads to the following $(r + N)$ th order approximation

$$\begin{bmatrix} \dot{T}_r \\ \dot{W} \\ Y \end{bmatrix} \approx \begin{bmatrix} A_{11}T_r + B_1U + R_{11}f_r(T_z, W, v), \\ g(T_z, W) \\ C_1T_r \end{bmatrix} \tag{21}$$

Since $T_z = [I \quad 0] Y$ from (16), it follows from the above that $T_z \approx C_r T_r$ where $C_r \triangleq [I \quad 0] C_1$. We now ignore the approximation errors and rewrite (21) as

$$\begin{bmatrix} \dot{T}_r \\ \dot{W} \\ Y \end{bmatrix} = \begin{bmatrix} A_{11}T_r + B_1U + R_{11}f_r(C_r T_r, W, v), \\ g(C_r T_r, W) \\ C_1T_r \end{bmatrix} \tag{22}$$

Eq. (22) is reduced order model (with state dimension $r + N$) of the full-scale system model (8) and (9).

The implicit assumption in the model reduction above is that the effect of the truncated $n - r$ states is not significant in the nonlinear term. Simulation results in next section suggest that this assumption holds well up to a particular order r of reduced model. Using the transformation $x_b = Rx$, given the initial temperature $T(0)$ and humidity ratio $W(0)$ of the full-scale model, initial value of the state $T_r(0)$ can be calculated as

$$T_r(0) = [R_{11} \quad R_{12}] T(0). \tag{23}$$

3.3. Non-dimensionalization

Before applying the technique developed in the previous section to the model (8)–(9) directly, the states and inputs need to be non-dimensionalized by appropriate scaling in order to achieve numerical robustness. To see the need for this, notice that the input vector U in (8) contains variables such as outside temperature (measured in °C) and heat gains from solar radiation and occupants (measured in W or kW), which differ significantly in magnitudes depending on the units of measurement used. For an LTI model $\dot{x} = Ax + Bu$, if two input signals have equal effect on the state but one has a much higher typical magnitude than the other,

the entry(-ies) of the B matrix corresponding to the larger input is likely to be smaller than those that correspond to the smaller input. In such a situation balanced truncation may incorrectly determine certain inputs to have little effect on the output. Effect of inputs on the outputs should not depend on the choice of units of measurements, and non-dimensionalizing the equations of the model before model reduction ameliorates such numerical issues. Non-dimensionalizing is a standard technique and its role in model reduction is probably known; though we were unable to find a reference for it.

We scale the variables T , T_0 , Q^s and Q^p as

$$\bar{T}_i = \frac{T_i}{T_i(0)}, \quad \bar{T}_0 = \frac{T_0}{T_{0\text{char}}}, \quad \bar{Q}_i^s = \frac{Q_i^s}{Q_{\text{char}}^s}, \quad \bar{Q}_i^p = \frac{Q_i^p}{Q_{\text{char}}^p}, \quad (24)$$

where $T_{0\text{char}}$ is the characteristic outside temperature, which is the average of maximum and minimum of the outside temperatures range expected, Q_{char}^s is the characteristic heat gain of a zone from solar radiation, and Q_{char}^p is the characteristic heat gain of a zone due to occupants. These are constants whose values can be set by the user. In the simulations reported later in Section 4, we used $T_{0\text{char}} = 27.5^\circ\text{C}$, $Q_{\text{char}}^s = 0.928\text{ kW}$ and $Q_{\text{char}}^p = 0.26\text{ kW}$. We now re-express (8) in terms of the non-dimensional variables defined above, to obtain

$$\dot{\bar{T}} = A_s \bar{T} + B_s \bar{U} + f_s(\bar{T}, W, \bar{v}) \quad (25)$$

where $\bar{U} \triangleq [\bar{T}_0, \bar{Q}_1^p, \dots, \bar{Q}_N^p, \bar{Q}_1^s, \dots, \bar{Q}_N^s]^T$, and \bar{v} is the scaled counterpart of v . Instead of applying balanced transformation to the LTI part of (8), it is applied to the LTI part of (25) and the transformation matrix R described in Section 3.2 is obtained. This new R matrix so obtained is used in the full-scale model defined in (25) and rest of procedure is same as described in Section 3.2.

4. Simulation results

Simulations are conducted for the four-zone building shown in Fig. 1. All four zones have an equal floor area of 25 m^2 , each wall is 5 m wide by 3 m tall. This provides a volumetric area of 75 m^3 for each zone. Zone 1 has a small window (5 m^2) on the north facing wall, whereas zones 2 and 4 have a larger window (7 m^2 each) on the east facing wall. Zone 3 does not have a window. All interior walls separating the zones have the same construction and all the exterior walls separating the zones from the outside have the same construction. All windows have the same resistance per unit area, $0.3\text{ (m}^2\text{ K/W)}$. It is assumed that the floor and the ceiling have the same construction as that of external wall, i.e., floor and ceiling have the same total thermal resistance and total capacitance per unit area as that of an exterior wall. The total thermal resistance per unit area of exterior wall and interior wall is chosen as $2.69\text{ (m}^2\text{ K/W)}$ and $0.45\text{ (m}^2\text{ K/W)}$, respectively. The total thermal capacitance per unit area of the exterior and interior walls is $493\text{ (kJ/(m}^2\text{ K))}$ and $52\text{ (kJ/(m}^2\text{ K))}$, respectively. These values are used in conjunction with the formulas in [6] to compute R and C values for the 3R2C models of the walls, the floor and the ceiling. The HVAC system used for both the buildings is designed to supply maximum flow rate of 0.25 kg/s per zone at the temperature of 12.8°C . These design choices were made after consulting with a HVAC expert. The number of people in a zone is chosen as a random integer that is uniformly distributed between 0 and 4. Outside temperature, outside humidity ratio and solar radiation data is obtained for a summer day (05/24/1996) of Gainesville, FL [32]. A proportional-integral (PI) controller for each zone is used in the full-scale model to determine the flow rates of conditioned air to track the desired zone temperature, which is set to 19°C for all the zones. All simulations reported here are open-loop simulations; the mass flow rates commanded by the PI controller are computed once using the full-scale model.

Table 1

Computation time vs. model order. The times reported here are the times taken by MATLAB 7.9.0 (R2009b) in running a simulation of the 4-zone building for 24 h in an Dell PC with a T3400 2.16GHz Intel Pentium Dual Duo processor.

	Model order	Computation time
Full-scale	40	189–397 s
Reduced	14	38–77 s
Maximally reduced	8	32–64 s

These flow rates are then used as inputs in conducting simulations with both the reduced order and full-scale model. This is done to ensure uniformity, especially in comparing simulation times. The inputs in the vector U are kept constant for every 10 min interval. All temperatures and humidity ratios are initialized at 24°C and 0.01, respectively. Inputs such as outside temperature, outside humidity ratio, mass flow rates and total internal heat gain for each zone are shown in Fig. 3.

Numerical results presented here are obtained from MATLAB simulations using the ode45 ODE solver. In figures and figure captions, superscript r represents the results obtained from reduced order model and legends 1, 2, 3 and 4 represent the results for the 1st, 2nd, 3rd and 4th zone, respectively. In particular, T_i^r and W_i^r are the temperature and humidity ratio of zone i predicted by a reduced order model. Correspondingly, $e_i^{(\text{Temp})} \triangleq T_i - T_i^r$ is the difference between the temperature of zone i predicted by the full-scale model and the reduced order model, while $e_i^{(W)} = W_i - W_i^r$ is the difference between the humidity ratio predicted by the full-scale model and the reduced order model.

The full-scale model for the four-zone building has 40 states. We tested two reduced order models for this system: (i) one with 14 states and (ii) one with 8 states. The minimum possible order using the proposed method is 8 since there are 4 zones. Figs. 4 and 5 show the zone temperatures and humidity ratios, respectively, for the 14th order reduced model. The rms error in the prediction is 0.5°C , which is of the same order as the spatial variation in temperature that exists inside a zone. The rms errors presented here is the one for that zone that has the maximum rms error among the four zones. The maximum error of 2.9°C appears during initial transients. The rms and maximum error in the humidity ratio predictions are 1.4×10^{-4} and 16×10^{-4} , which are 1.6% and 18% of the predictions by the full-scale model, respectively. Again, the maximum error occurs in the first 20 min due to initial condition mismatches. After that the error is around 1%. We believe that the large initial error is due to the difference between the initial conditions of the reduced order and the full-scale model, which occurs due to the transformation (23).

Predictions by the 8th order reduced model are shown in Figs. 6 and 7. Temperature predictions by the 8th order reduced model show larger error in both transient and steady state behavior compared to the 14th order model; cf. Fig. 4. It is known that reducing the model order increases the prediction errors due to the truncation of states corresponding to the large values. Therefore, the rms and maximum error in the temperature predictions are 2°C and 9.7°C when the model order is reduced to 8. However, the error in the humidity ratio predictions are similar to the 14th order case: the rms and maximum errors are 1.39×10^{-4} (i.e., 1.6%) and 16×10^{-4} (i.e., 18%). It seems to suggest that the effect of temperature variation on humidity ratio is small, and that model order has less effect on humidity than on temperature. These comparisons also illustrate the compromise between prediction accuracy and reduction in model order.

Table 1 presents a comparison between the computation times and model order. The table shows a speed-up of computation time by a factor of 6 when the model order is reduced by a factor of 5 (from 40 to 8). In simulations conducted with a 2316 state model

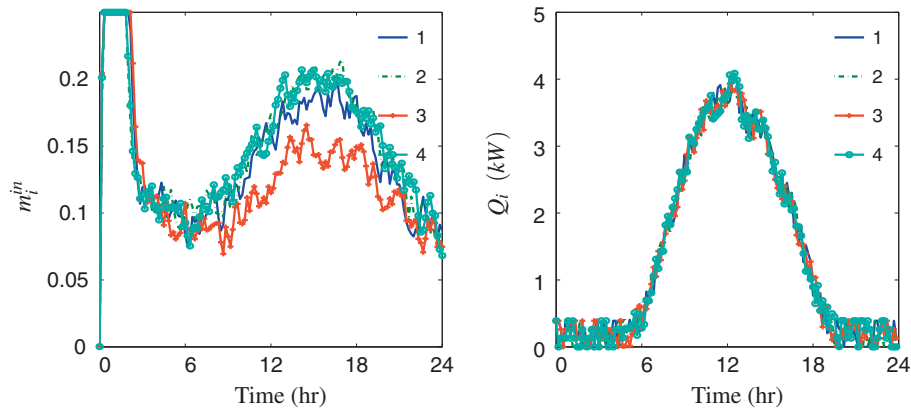


Fig. 3. Input signals: mass flow rates (m_i^{in}) and total internal heat gain $Q_i (= Q_i^s + Q_i^p)$ in each zone for a four-zone building, $i = 1, 2, \dots, 4$.

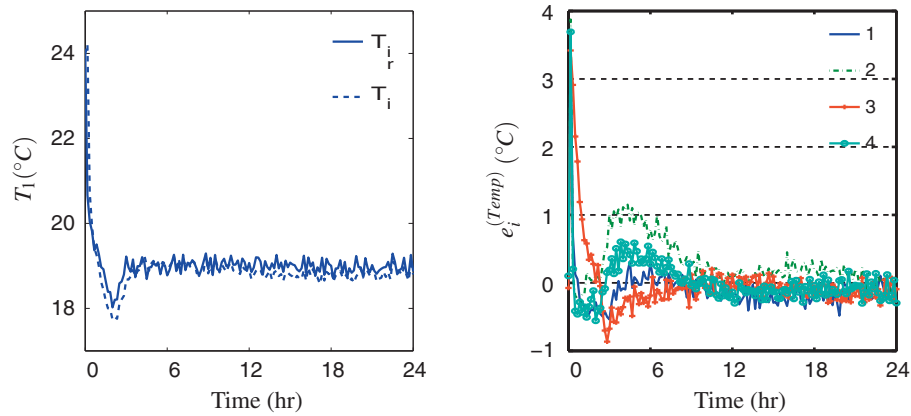


Fig. 4. Performance with intermediate reduction in model order: (left) temperature in zone 1 and (right) difference in temperatures between full-scale 40th order and reduced 14th order model for a four-zone building, $i = 1, 2, \dots, 4$. Recall that $e_i^{(Temp)} = T_i - T_i^r$ where the superscript r corresponds to the reduced order model.

(for a building with 66 zones) the speed-up factor is observed to be 12 when the model order is reduced to the minimum possible value, namely, 132.

5. Conclusion

This paper presents a method for model reduction of a class of non-linear systems that models the thermal dynamics in a multi-zone building. The full-scale model of the building thermal

dynamics, which is itself a lumped parameter model, has a larger number of states even for a moderate number of zones. Since the full-scale model is non-linear, there are very few existing model reduction methods that are applicable. The ones that are applicable do not exploit the special structure of building thermal dynamics, while the proposed method, by exploiting this structure, extends tools from linear model reduction to a non-linear problem. The proposed technique is seen to work very well in simulations—the prediction of the zone temperatures and humidities are quite close

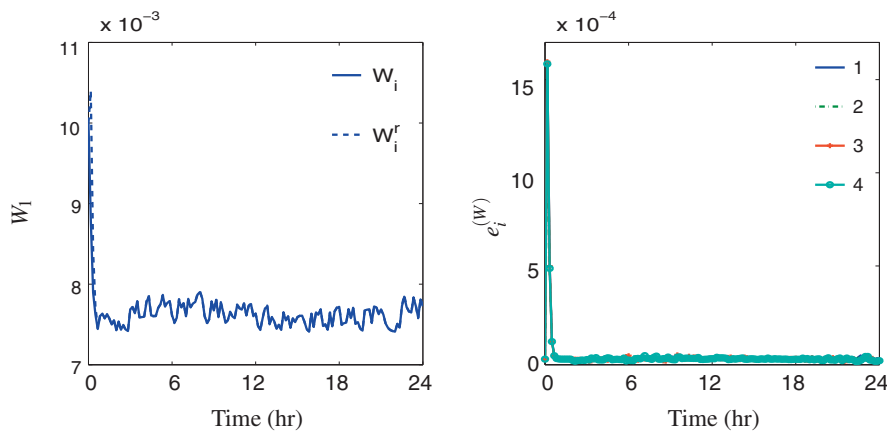


Fig. 5. Performance with intermediate reduction in model order: (left) humidity ratio in zone 1 and (right) difference in humidity ratios between full-scale 40th order model and reduced 14th order model for zones $i = 1, 2, \dots, 4$. Recall that $e_i^{(W)} = W_i - W_i^r$ where the superscript r corresponds to the reduced order model.

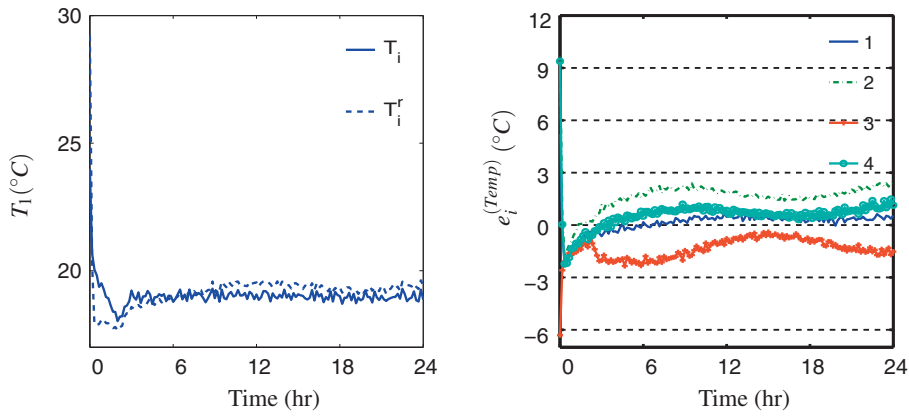


Fig. 6. Performance with maximum reduction in model order: (left) temperature in zone 1 and (right) difference in temperatures between full-scale 40th order and reduced 8th order model for zones $i=1, 2, \dots, 4$. Recall that $e_i^{(Temp)} = T_i - T_i^r$ where the superscript r corresponds to the reduced order model.

to the predictions of the full-scale model even when the model order is reduced to the minimum possible. The maximum errors are seen for a short period of time in the initial transient phase, which occurs due to mismatches in the initial conditions. Afterwards the errors in temperature and humidity predictions remain small. Temperature prediction accuracy seems to be more sensitive to model order than humidity ratio. It is observed that appropriate scaling of the states of the full-scale model, before applying the reduction method, is crucial for the reduced model to retain prediction accuracy.

The proposed model reduction method is applicable as long as the full-scale model has the specific sparsity structure as that of (8) and (9). Since the full-scale model is based on basic mass and heat balance, we expect the model to be applicable to a wide range of building systems. One situation where we suspect this modeling framework may not be applicable is when there is significant convection between the zones, which happens in building that rely only on natural ventilation. In these cases some of the assumption made in constructing the full-scale model do not hold. In particular, the assumption that the temperature and humidity of the air entering a zone are determined solely by the AHU and do not depend on the temperature and humidity of air at any other zone may be violated. However, the model reduction method may still be applicable as long as the full-scale thermal model has the same structure as that of (8) and (9).

Since the number of outputs of the model is twice the number of zones, the minimum order of the reduced model achievable by this method is also twice the number of zones. A future area of research is to enable further order reduction. For instance, it may be beneficial to be able to reduce the model of a building with a large number of zones into a model with just a few “super zones”. Such a reduction will also provide insight into the design of the building, since it will club together zones that interact strongly with one another into a super zone. The model reduction method proposed in [19] for the linear part of the model (the RC-network portion) is capable of doing that. Work is ongoing in integrating the method proposed here and the one in [19] to obtain a method that can identify super-zones and can also handle the non-linear part of the dynamics.

In constructing the full-scale model we have ignored convective thermal interaction among zones since simplified models of such interaction that are of sufficient accuracy are lacking. An important area of research for building thermal modeling is constructing reduced order models of inter-zone convective heat transfer. Preliminary work in identifying reduced order RC network models of inter-zone convection is reported in [10]. If the full-scale model is augmented with such convection sub-models, the proposed model reduction method can be directly applied. The reason is that coupling additional RC networks to the full-scale model does not change its structural properties that the proposed method exploits.

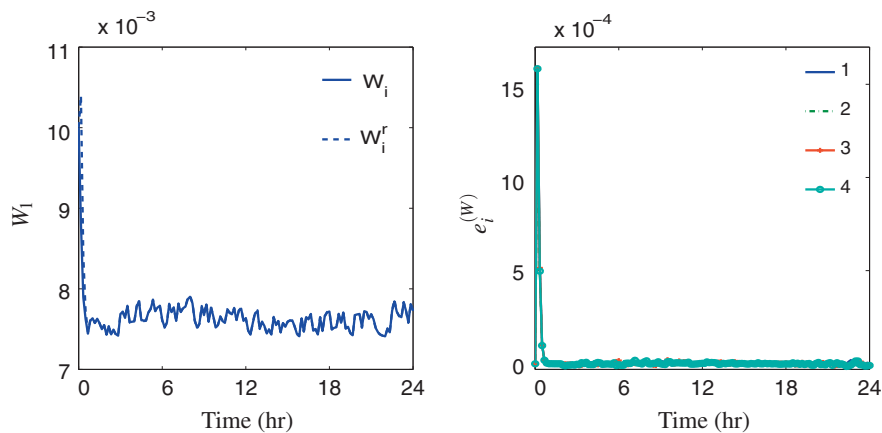


Fig. 7. Performance with maximum reduction in model order: (left) humidity ratio in zone 1 and (right) difference in humidity ratios between full-scale 40th order model and reduced 8th order model for zones $i=1, 2, \dots, 4$. Recall $e_i^{(W)} = W_i - W_i^r$ where the superscript r corresponds to the reduced order model.

However, other forms of lumped convection models may require further research in model reduction.

Acknowledgments

The authors gratefully acknowledge Prof. H.H. Ingley's help in choosing the four-zone building parameters and its HVAC system design, and thank Prof. Prashant Mehta for several helpful discussions.

Appendix A. Derivation of (7)

The humidity ratio W of a zone is defined as

$$W := \frac{M_w}{M_{da}}, \quad (\text{A.1})$$

where M_w is the mass of water vapor and M_{da} is the mass of dry air in the zone. Differentiating (A.1) with respect to time gives us

$$\begin{aligned} \dot{W} &= \frac{d}{dt} \left[\frac{M_w}{M_{da}} \right] = \frac{\dot{M}_w M_{da} - M_w \dot{M}_{da}}{M_{da}^2} = \frac{1}{M_{da}} (\dot{M}_w - W \dot{M}_{da}) \\ &= \frac{1}{V_{da} \rho_{da}} (\dot{M}_w - W \dot{M}_{da}) \end{aligned} \quad (\text{A.2})$$

where V_{da} is the volume of dry air (which is same as the zone volume V), and ρ_{da} is the density of dry air. It is known from the ideal gas law that $\rho_{da} = \frac{p_{da}}{R_g T}$, where p_{da} is the partial pressure of dry air, T is the air temperature, and R_g is the specific gas constant of dry air. Equation (A.2) can now be rewritten as

$$\dot{W} = \frac{R_g T}{V p_{da}} (\dot{M}_w - W \dot{M}_{da}) \quad (\text{A.3})$$

Ignoring infiltration and exfiltration into and out of the zone, the mass flow rate of air leaving a zone (m^{out}) can be decomposed into dry air mass flow rate and water vapor mass flow rate as

$$m^{\text{out}} = m_{da}^{\text{out}} + m_w^{\text{out}}, \quad (\text{A.4})$$

where m_{da}^{out} and m_w^{out} are rates of dry air and water vapor rates leaving the zone, respectively. We can rewrite (A.4) as

$$m^{\text{out}} = (1 + W^{\text{out}}) m_{da}^{\text{out}} = (1 + W) m_{da}^{\text{out}} \quad (\text{A.5})$$

where W^{out} is the humidity ratio of the air leaving the zone, and we have assumed that the humidity ratio of air in the zone is same as the humidity ratio of air going out of the zone. Similarly, flow rate of air entering the zone (m^{in}) can be written as

$$m^{\text{in}} = (1 + W^{\text{in}}) m_{da}^{\text{in}} \quad (\text{A.6})$$

where m_{da}^{in} is the flow rate of dry air entering the zone and W^{in} is the humidity ratio of the air entering the zone. The following equations follow from mass balance:

$$\dot{M}_w = n^p \omega_{\text{H}_2\text{O}} + m_w^{\text{in}} - m_w^{\text{out}}, \quad \dot{M}_{da} = m_{da}^{\text{in}} - m_{da}^{\text{out}} \quad (\text{A.7})$$

where m_w^{in} is the flow rate of water vapor entering the zone. Eqs. (A.5) and (A.6) can be rearranged to provide

$$\begin{aligned} m_{da}^{\text{out}} &= \frac{1}{1 + W} m^{\text{out}}, & m_w^{\text{out}} &= \frac{W}{1 + W} m^{\text{out}}, \\ m_{da}^{\text{in}} &= \frac{1}{1 + W^{\text{in}}} m^{\text{in}}, & m_w^{\text{in}} &= \frac{W^{\text{in}}}{1 + W^{\text{in}}} m^{\text{in}} \end{aligned} \quad (\text{A.8})$$

Combining (A.8) and (A.7) with (A.3) leads to

$$\dot{W} = \frac{R_g T}{V p_{da}} \left[n^p \omega_{\text{H}_2\text{O}} + m^{\text{in}} \frac{W^{\text{in}} - W}{1 + W^{\text{in}}} \right]. \quad (\text{A.9})$$

Eq. (7) is simply (A.9) applied to each zone.

References

- [1] F. Oldewurtel, A. Parisio, C. Jones, M. Morari, D. Gyalistras, M. Gwerder, V. Stauch, B. Lehmann, K. Wirth, Energy efficient building climate control using stochastic model predictive control and weather predictions, in: American Control Conference, 2010, pp. 5100–5105.
- [2] D. Gyalistras, M. Gwerder, Use of weather and occupancy forecasts for optimal building climate control (opticontrol): two years progress report, Tech. rep., Siemens Switzerland Ltd., 2010.
- [3] P. Morosan, R. Bourdais, D. Dumur, A distributed MPC strategy based on benders decomposition applied to multi-source multi-zone temperature regulation, *Journal of Process Control* 21 (2011) 729–737.
- [4] M. Mossolli, K. Ghalib, N. Ghaddar, Optimal control strategy for a multi-zone air conditioning system using a genetic algorithm, *Energy* 34 (1) (2009) 58–66, doi:10.1016/j.energy.2008.10.001.
- [5] X. Xu, S. Wang, Z. Sun, F. Xiao, A model-based optimal ventilation control strategy of multi-zone VAV air-conditioning systems, *Applied Thermal Engineering* 29 (1) (2009) 91–104, doi:10.1016/j.applthermaleng.2008.02.017.
- [6] M. Gouda, S. Danaher, C. Underwood, Building thermal model reduction using nonlinear constrained optimization, *Building and Environment* 37 (2002) 1255–1265.
- [7] M. Gouda, S.D.C. Underwood, Low-order model for the simulation of a building and its heating system, *Building Services Energy Research Technology* 21 (2000) 199–208.
- [8] T. Nielsen, Simple tool to evaluate energy demand and indoor environment in the early stages of building design, *Solar Energy* 78 (2005) 73–83.
- [9] ASHRAE, The ASHRAE Handbook Fundamentals, SI ed., 2005.
- [10] S. Goyal, C. Liao, P. Barooah, Identification of multi-zone building thermal interaction model from data, to be presented at the IEEE Conf. on Decision and Control, December 2011.
- [11] A.C. Antoulas, D.C. Sorensen, S. Gugercin, A survey of model reduction methods for large-scale systems, *Contemporary Mathematics* 280 (2001) 193–219.
- [12] S. Al-Baiyat, M.B.U. Al-Saggaf, New model reduction scheme for bilinear systems, *International Journal of Systems Science* 25 (1994) 1631–1642.
- [13] S. Al-Baiyat, M. Bettayeb, A new model reduction scheme for k-power bilinear systems, in: 32nd IEEE Conference on Decision and Control, Vol. 1, 1993, pp. 22–27.
- [14] W. Gray, J. Mesko, Energy functions and algebraic Gramians for bilinear systems, in: 4th IFAC Nonlinear Control Systems Design Symposium, 1998.
- [15] L. Zhang, J. Lam, On h_2 model reduction of bilinear systems, *Automatica* 38 (2002) 205–216.
- [16] J. Scherpen, Balancing for nonlinear systems, *Systems and Control Letters* 21 (1993) 143–153.
- [17] S. Lall, J. Marsden, S. Glavaski, A subspace approach to balanced truncation for model reduction of nonlinear control systems, *Journal of Robust and Nonlinear Control* 12 (2002) 519–526.
- [18] J. Hahn, T. Edgar, An improved method for nonlinear model reduction using balancing of empirical Gramians, *Computers and Chemical Engineering* 26 (2002) 1379–1397.
- [19] K. Deng, P. Barooah, P. Mehta, S. Meyn, Building thermal model reduction via aggregation of states, in: American Control Conference, 2010, pp. 5118–5123.
- [20] B. Tashtoush, M. Molhim, Dynamic model of an HVAC system for control analysis, *Energy* 30 (2005) 1729–1745.
- [21] S. Wang, X. Xu, Simplified building model for transient thermal performance estimation using GA-based parameter identification, *International Journal of Thermal Sciences* 45 (2006) 419–432.
- [22] R. Yao, N. Baker, M. McEvoy, A simplified thermal resistance network model for building thermal simulation, in: The Canadian Conference on Building Energy Simulation (eSim'02), 2002.
- [23] M. Zaheer-Uddin, G. Zheng, A dynamic model of a multizone VAV system for control analysis, *Transactions- American Society of Heating Refrigerating and Air Conditioning Engineers* 100 (1994) 219.
- [24] J. Kampf, D. Robinson, A simplified thermal model to support analysis of urban resource flows, *Energy and Buildings* 39 (2007) 445–453.
- [25] S. Wang, Dynamic simulation of building VAV air-conditioning system and evaluation of EMCs on-line control strategies, *Building and Environment* 36 (1999) 681–705.
- [26] J. Bourdouxhe, M. Grodent, J. Lebrun, Reference guide for dynamic models of HVAC equipment, ASHRAE, 1998.
- [27] M. Turner, D. Bates (Eds.), *Mathematical Methods for Robust and Nonlinear Control*, 1st ed., Springer, 2007.
- [28] M. Dahleh, M. Dahleh, G. Verghese, *Lectures on Dynamic Systems and Control*, 1999, <http://ocw.mit.edu/index.htm>.
- [29] K. Zhou, J. Doyle, *Essentials of robust control*, Prentice Hall, 1998.
- [30] U. Mackenroth, *Robust Control Systems: Theory and Case Studies*, Springer, 2004.
- [31] National Solar Radiation Data Base (NSRDB), 2005, http://rredc.nrel.gov/solar/old_data/nsrdb/1991-2005/tmy3/.